CONJUGATE GRADIENT–BOUNDARY ELEMENT METHOD FOR THE CAUCHY PROBLEM IN ELASTICITY

by L. MARIN

(*Department of Applied Mathematics, University of Leeds, Leeds* LS2 9JT)

DINH NHO HÀO

(*Hanoi Institute of Mathematics, PO Box* 631*, Bo Ho,* 10000 *Hanoi, Vietnam*)

and D. LESNIC

(*Department of Applied Mathematics, University of Leeds, Leeds* LS2 9JT)

[Received 28 August 2000. Revise 6 August 2001]

Summary

In this paper, an iterative algorithm based on the conjugate gradient method (CGM) in combination with the boundary element method (BEM) for obtaining stable approximate solutions to the Cauchy problem in linear elasticity is analysed. An efficient stopping criterion for the CGM proposed by Nemirovskii in 1986 is employed and in addition the accuracy of the iterative algorithm is improved by using a variable relaxation procedure. The numerical results obtained confirm that the iterative BEM produces a convergent and stable numerical solution with respect to increasing the number of boundary elements and decreasing the amount of noise added into the input data.

1. Introduction

In most boundary-value problems in solid mechanics, the governing system of equations (equilibrium, constitutive and kinematics equations) has to be solved with the appropriate initial and boundary conditions for the traction and/or displacement vectors (Dirichlet, Neumann or mixed boundary conditions). These are called *direct problems* and their existence and uniqueness have been well established. Unfortunately, many engineering problems do not belong to this category. In particular, the boundary conditions are often incomplete, either in the form of underspecified and overspecified boundary conditions on different parts of the boundary or the solution is prescribed at some internal points in the domain. These are inverse problems, and it is well known that they are generally ill-posed so that the existence, uniqueness and stability of their solutions are not always guaranteed.

Much of the literature on the solution of inverse problems has been devoted to inverse heat transfer (**1**), whilst research in the field of inverse elasticity has been limited. Inverse deformation problems have also been discussed in the field of thermoelasticity by Grysa *et al.* (**2**) and for non-destructive measurements of plastic strains by Mura (**3**). Maniatty *et al.* (**4**) used simple diagonal regularization, in conjunction with the finite element method (FEM), to determine the traction boundary condition. Spatial regularization was introduced in conjunction with the boundary element

 © Oxford University Press 2002

method (BEM) in (**5**) and with the FEM in (**6**). Ikehata (**7**) showed that the material constants can be determined in the case of Love–Kirchhoff plate theory by using the Dirichlet-to-Neumann map, whilst Zhang *et al.* (**8**) used constraint least-squares minimization to determine the residual stress and contact pressure. Recently, Shi and Mukherjee (**9**) have studied the shape optimization of a three-dimensional linear elastic body using a variant of the BEM, namely the boundary contour method. Other inverse problems for differential equations of elasticity can be found in (**10**, **11**).

In this paper we apply a variational method for solving the Cauchy problem in two-dimensional elasticity by considering the displacement on the underspecified boundary as a control in a direct mixed well-posed problem while trying to fit the Cauchy data on the overspecified boundary. In doing so we attempt to minimize a functional relating the discrepancies between the known and calculated values of the displacement on the overspecified boundary following a technique similar to that used in (**12**) for the Cauchy problem for the Laplace equation. We prove that this functional is twice Fréchet differentiable and a formula for the gradient of the functional is obtained via some appropiate adjoint problems. Since the minimization problem contains almost all the properties of the Cauchy problem it still remains ill-posed. The conjugate gradient method (CGM), with a stopping rule proposed by Nemirovskii (**13**), is therefore employed. This method is known to have an optimal-order convergence rate (**13**). The numerical implementation of the CGM is based on the BEM following a technique similar to that used in (**14**) for an inverse problem in which discrete data measurements of the displacement at internal points are used to determine the underspecified boundary data.

2. Cauchy problem in linear elasticity

Consider a linear elastic material which occupies an open bounded domain $\Omega \subset \mathbb{R}^d$, where d is the dimension of the space in which the problem is posed, usually $d \in \{1, 2, 3\}$, and assume that Ω is bounded by a surface $\Gamma = \partial\Omega \in C^1$. We also assume that the boundary consists of two parts, $\Gamma = \Gamma_1 \cup \Gamma_2$, where $\Gamma_1, \Gamma_2 \neq \emptyset$ and $\Gamma_1 \cap \Gamma_2 = \emptyset$. In the absence of body forces, the equilibrium equations for $d = 3$ are given by (**15**)

$$\partial_j \sigma_{ij}(\boldsymbol{u}(\boldsymbol{x})) = 0, \qquad \boldsymbol{x} \in \Omega, \tag{1}$$

where $\partial_j \equiv \partial/\partial x_j$, σ_{ij} is the stress tensor and the strain tensor ε_{ij} is given by the kinematic relations

$$\varepsilon_{ij}(\boldsymbol{u}(\boldsymbol{x})) = \tfrac{1}{2}(\partial_j u_i(\boldsymbol{x}) + \partial_i u_j(\boldsymbol{x})). \tag{2}$$

These tensors are related by the constitutive law, namely

$$\sigma_{ij}(\boldsymbol{u}(\boldsymbol{x})) = C_{ijkl}\varepsilon_{kl}(\boldsymbol{u}(\boldsymbol{x})), \tag{3}$$

where C_{ijkl} is the elasticity tensor which, for an isotropic material, is given by

$$C_{ijkl} = G\{2\nu(1-2\nu)^{-1}\delta_{ij}\delta_{kl} + \delta_{ik}\delta_{jl} + \delta_{il}\delta_{jk}\}. \tag{4}$$

Here G is the shear modulus, ν is Poisson's ratio and δ_{ij} is the Kronecker delta.

If we now substitute (3) into (1), and use (2) and (4), we obtain the Lamé system

$$G\frac{\partial^2 u_i(\boldsymbol{x})}{\partial x_j \partial x_j} + \frac{G}{1-2\nu}\frac{\partial^2 u_j(\boldsymbol{x})}{\partial x_i \partial x_j} = 0, \qquad \boldsymbol{x} \in \Omega. \tag{5}$$

We now let $\boldsymbol{n}(\boldsymbol{x})$ be the outward normal vector at Γ and $\boldsymbol{t}(\boldsymbol{x})$ be the traction vector at a point $\boldsymbol{x} \in \Gamma$ whose components are defined by $t_i(\boldsymbol{x}) = \sigma_{ij}(\boldsymbol{u}(\boldsymbol{x}))n_j(\boldsymbol{x})$. In the direct problem formulation, the knowledge of the displacement and/or traction vectors on the whole boundary Γ gives the corresponding Dirichlet, Neumann, or mixed boundary conditions which enables us to determine $\boldsymbol{u}$ in Ω. Then, ε_{ij} can be calculated from (2) and the stress tensor is determined using (3).

Assuming that both $\boldsymbol{u}$ and $\boldsymbol{t}$ can be measured on a part of Γ, say Γ_2, leads to the mathematical formulation of an inverse problem consisting of (1) or (5) and the boundary conditions

$$u_i(\boldsymbol{x}) = \widetilde{u}_i(\boldsymbol{x}), \qquad t_i(\boldsymbol{x}) = \widetilde{t}_i(\boldsymbol{x}), \qquad \boldsymbol{x} \in \Gamma_2, \tag{6}$$

where $\widetilde{\boldsymbol{u}}$ and $\widetilde{\boldsymbol{t}}$ are prescribed vector-valued functions. In the above formulation of the boundary conditions (6), it can be seen that Γ_2 is overspecified by prescribing both the displacement $\boldsymbol{u}_{|\Gamma_2} = \widetilde{\boldsymbol{u}}$ and the traction $\boldsymbol{t}_{|\Gamma_2} = \widetilde{\boldsymbol{t}}$ vectors, whilst Γ_1 is underspecified since both $\boldsymbol{u}_{|\Gamma_1}$ and $\boldsymbol{t}_{|\Gamma_1}$ are unknown and have to be determined.

This problem, termed a Cauchy problem, is much more difficult to solve both analytically and numerically than the direct problem, since the solution does not satisfy the general conditions of well-posedness. Although the problem may have a unique solution, it is well known (**16**) that this solution is unstable with respect to small perturbations in the data on Γ_2. Thus the problem is ill-posed and we cannot use a direct approach, such as the Gauss elimination method, in order to solve the system of linear equations which arises from the discretization of the partial differential equations (1) or (5) and the boundary conditions (6). Therefore, knowing the data $\widetilde{\boldsymbol{u}}$ and $\widetilde{\boldsymbol{t}}$ on the boundary Γ_2, we apply a variational method to the aforementioned Cauchy problem. Since the boundary conditions on Γ_1 are unknown and have to be determined, we consider the displacement vector on the underspecified boundary Γ_1 as a control for a direct problem and attempt to fit the Cauchy data on the overspecified boundary Γ_2 by minimizing a functional relating the known and calculated values of the displacement vector on Γ_2.

3. Variational formulation

Let us denote by $\mathbb{L}^2(\Gamma_i)$, $\mathbb{H}^s(\Gamma_i)$ and $\mathbb{H}^s(\Omega)$ the spaces $(L^2(\Gamma_i))^d$, $(H^s(\Gamma_i))^d$ and $(H^s(\Omega))^d$, respectively, for $d \in \{1, 2, 3\}$, $i = 1, 2$ and some $s \in \mathbb{R}$. Then the Cauchy problem under investigation is given by (1) and (6), where $\widetilde{\boldsymbol{u}} \in \mathbb{L}^2(\Gamma_2), \widetilde{\boldsymbol{t}} \in \mathbb{L}^2(\Gamma_2)$ and $\boldsymbol{u}$ is sought in $\mathbb{H}^{1/2}(\Omega)$. We note that $\widetilde{\boldsymbol{t}} \in \mathbb{H}^{-1}(\Gamma_2)$ is sufficient for our method. Let us denote by $\gamma_i f$ the trace of a function f determined in Ω over Γ_i, $i = 1, 2$. First we solve the direct problem

$$\left.\begin{aligned} &\partial_j \sigma_{ij}(\boldsymbol{u}(\boldsymbol{x})) = 0, && \boldsymbol{x} \in \Omega, \\ &\gamma_1 u_i(\boldsymbol{x}) = v_i(\boldsymbol{x}), && \boldsymbol{x} \in \Gamma_1, \\ &\gamma_2(\sigma_{ij}(\boldsymbol{u}(\boldsymbol{x}))n_j(\boldsymbol{x})) = \widetilde{t}_i(\boldsymbol{x}), && \boldsymbol{x} \in \Gamma_2, \end{aligned}\right\} \tag{7}$$

with $\boldsymbol{v} \in \mathbb{L}^2(\Gamma_1)$. We denote by $\boldsymbol{u} = \boldsymbol{u}(\boldsymbol{v}, \widetilde{\boldsymbol{t}})$ the solution to the problem (7) and aim to find $\boldsymbol{v} \in \mathbb{L}^2(\Gamma_1)$ such that

$$A\boldsymbol{v} := \gamma_2 \boldsymbol{u}(\boldsymbol{v}, \widetilde{\boldsymbol{t}}) = \widetilde{\boldsymbol{u}}. \tag{8}$$

To do so, we attempt to minimize the functional

$$J(\boldsymbol{v}) = \tfrac{1}{2}\|A\boldsymbol{v} - \widetilde{\boldsymbol{u}}\|_{\mathbb{L}^2(\Gamma_2)} \tag{9}$$

with respect to $\boldsymbol{v} \in \mathbb{L}^2(\Gamma_1)$.

We note that since $\boldsymbol{v} \in \mathbb{L}^2(\Gamma_1)$, $\widetilde{\boldsymbol{t}} \in \mathbb{L}^2(\Gamma_2)$ and the boundary $\Gamma \in C^1$, there is a unique solution $\boldsymbol{u}(\boldsymbol{v}, \widetilde{\boldsymbol{t}}) \in \mathbb{H}^{1/2}(\Omega)$ of the direct problem (7) (see (**17**, Chapter 2, section 7.3)). Thus, $A\boldsymbol{v} = \gamma_2 \boldsymbol{u}(\boldsymbol{v}, \widetilde{\boldsymbol{t}}) \in \mathbb{L}^2(\Gamma_1)$ and hence expression (8) is meaningful.

In what follows we need the following result on Green's formula: for $\boldsymbol{p} \in \mathbb{L}^2(\Gamma_2)$, consider the problem

$$\left.\begin{aligned} &\partial_j \sigma_{ij}(\boldsymbol{\psi}(\boldsymbol{x})) = 0, && \boldsymbol{x} \in \Omega, \\ &\gamma_1 \psi_i(\boldsymbol{x}) = 0, && \boldsymbol{x} \in \Gamma_1, \\ &\gamma_2(\sigma_{ij}(\boldsymbol{\psi}(\boldsymbol{x}))n_j(\boldsymbol{x})) = p_i(\boldsymbol{x}), && \boldsymbol{x} \in \Gamma_2. \end{aligned}\right\} \tag{10}$$

LEMMA 1. *Let* $\boldsymbol{u}$ *and* $\boldsymbol{\psi}$ *be the solutions of problems* (7) *and* (10)*, respectively. Then*

$$\int_{\Gamma_1} \gamma_1(\sigma_{ij}(\boldsymbol{\psi}(\boldsymbol{x}))n_j(\boldsymbol{x}))v_i(\boldsymbol{x})\, d\Gamma(\boldsymbol{x}) + \int_{\Gamma_2} p_i(\boldsymbol{x})\gamma_2 u_i(\boldsymbol{x})\, d\Gamma(\boldsymbol{x}) = \int_{\Gamma_2} \widetilde{t}_i(\boldsymbol{x})\gamma_1\psi_i(\boldsymbol{x})\, d\Gamma(\boldsymbol{x}). \tag{11}$$

Proof. We note that if $\boldsymbol{p} \in \mathbb{L}^2(\Gamma_2)$, then $\boldsymbol{\psi} \in \mathbb{H}^{3/2}(\Omega)$ and hence $\gamma_1(\sigma_{ij}(\boldsymbol{\psi}(\boldsymbol{x}))n_j(\boldsymbol{x})) \in \mathbb{L}^2(\Gamma_1)$. It follows that (11) is meaningful in the classical sense. This can be proved in the framework of distribution theory (see (**17**, Chapter 2, section 2.2)) but an alternative proof is given here.

Let $\boldsymbol{v}^{(n)} \in \mathbb{H}^1(\Gamma_1)$ be a sequence which converges to $\boldsymbol{v}$ in the $\mathbb{L}^2(\Gamma_1)$-norm. We denote by $\boldsymbol{u}^{(n)} = \boldsymbol{u}(\boldsymbol{v}^{(n)}, \widetilde{\boldsymbol{t}})$ the solution of problem (7) with $\boldsymbol{v} = \boldsymbol{v}^{(n)}$. It can be proved (see (**17**, Chapter 2, section 7.3)) that $\boldsymbol{u}^{(n)} \in \mathbb{H}^{3/2}(\Omega)$ and $\boldsymbol{u}^{(n)} \to \boldsymbol{u}$ in $\mathbb{H}^{1/2}(\Omega)$. It follows that $\gamma_2 u_i^{(n)} \to \gamma_2 u_i$ in $\mathbb{L}^2(\Gamma_2)$. Since $\boldsymbol{\psi} \in \mathbb{H}^{3/2}(\Omega)$ and using (2) and (3), we have

$$\begin{aligned} 0 &= \int_\Gamma \sigma_{ij}(\boldsymbol{u}^{(n)}(\boldsymbol{x}))n_j(\boldsymbol{x})\psi_i(\boldsymbol{x})\, d\Gamma(\boldsymbol{x}) - \int_\Omega \sigma_{ij}(\boldsymbol{u}^{(n)}(\boldsymbol{x}))\varepsilon_{ij}(\boldsymbol{\psi}(\boldsymbol{x}))\, d\Omega(\boldsymbol{x}) \\ &= \int_{\Gamma_1} \gamma_1(\sigma_{ij}(\boldsymbol{u}^{(n)}(\boldsymbol{x}))n_j(\boldsymbol{x}))\, \gamma_1\psi_i(\boldsymbol{x})\, d\Gamma(\boldsymbol{x}) + \int_{\Gamma_2} \gamma_2(\sigma_{ij}(\boldsymbol{u}^{(n)}(\boldsymbol{x}))n_j(\boldsymbol{x}))\, \gamma_2\psi_i(\boldsymbol{x})\, d\Gamma(\boldsymbol{x}) \\ &\quad - \int_\Omega C_{ijkl}\varepsilon_{kl}(\boldsymbol{u}^{(n)}(\boldsymbol{x}))\varepsilon_{ij}(\boldsymbol{\psi}(\boldsymbol{x}))\, d\Omega(\boldsymbol{x}). \end{aligned} \tag{12}$$

If we now substitute the boundary conditions from both problems (7) and (10) into the surface integrals in (12), we obtain

$$\int_\Omega C_{ijkl}\varepsilon_{kl}(\boldsymbol{u}^{(n)}(\boldsymbol{x}))\varepsilon_{ij}(\boldsymbol{\psi}(\boldsymbol{x}))\, d\Omega(\boldsymbol{x}) = \int_{\Gamma_2} \widetilde{t}_i(\boldsymbol{x})\gamma_2\psi_i(\boldsymbol{x})\, d\Gamma(\boldsymbol{x}). \tag{13}$$

In a similar manner, since $\boldsymbol{u}^{(n)} \in \mathbb{H}^{3/2}(\Omega)$ and using (2) and (3), we have

$$\begin{aligned} 0 &= \int_\Gamma \sigma_{ij}(\boldsymbol{\psi}(\boldsymbol{x}))n_j(\boldsymbol{x})u_i^{(n)}(\boldsymbol{x})\, d\Gamma(\boldsymbol{x}) - \int_\Omega \sigma_{ij}(\boldsymbol{\psi}(\boldsymbol{x}))\varepsilon_{ij}(\boldsymbol{u}^{(n)}(\boldsymbol{x}))\, d\Omega(\boldsymbol{x}) \\ &= \int_{\Gamma_1} \gamma_1(\sigma_{ij}(\boldsymbol{\psi}(\boldsymbol{x}))n_j(\boldsymbol{x}))\, \gamma_1 u_i^{(n)}(\boldsymbol{x})\, d\Gamma(\boldsymbol{x}) + \int_{\Gamma_2} \gamma_2(\sigma_{ij}(\boldsymbol{\psi}(\boldsymbol{x}))n_j(\boldsymbol{x}))\, \gamma_2 u_i^{(n)}(\boldsymbol{x})\, d\Gamma(\boldsymbol{x}) \\ &\quad - \int_\Omega C_{ijkl}\varepsilon_{kl}(\boldsymbol{\psi}(\boldsymbol{x}))\varepsilon_{ij}(\boldsymbol{u}^{(n)}(\boldsymbol{x}))\, d\Omega(\boldsymbol{x}). \end{aligned} \tag{14}$$

Using the boundary conditions from (7) and (10) in (14) gives

$$\int_\Omega C_{ijkl}\varepsilon_{kl}(\boldsymbol{\psi}(\boldsymbol{x}))\varepsilon_{ij}(\boldsymbol{u}^{(n)}(\boldsymbol{x}))\,d\Omega(\boldsymbol{x}) = \int_{\Gamma_1}\gamma_1(\sigma_{ij}(\boldsymbol{\psi}(\boldsymbol{x}))n_j(\boldsymbol{x}))v_i^{(n)}(\boldsymbol{x})\,d\Gamma(\boldsymbol{x}) + \int_{\Gamma_2} p_i(\boldsymbol{x})\gamma_2 u_i^{(n)}(\boldsymbol{x})\,d\Gamma(\boldsymbol{x}). \quad (15)$$

From the symmetry properties of the elasticity tensor C_{ijkl} (**15**), it follows that

$$C_{ijkl}\,\varepsilon_{kl}(\boldsymbol{u}^{(n)}(\boldsymbol{x}))\varepsilon_{ij}(\boldsymbol{\psi}(\boldsymbol{x})) = C_{ijkl}\,\varepsilon_{kl}(\boldsymbol{\psi}(\boldsymbol{x}))\varepsilon_{ij}(\boldsymbol{u}^{(n)}(\boldsymbol{x}))$$

and, therefore, the domain integrals in (13) and (15) are equal. Consequently, we have

$$\int_{\Gamma_1}\gamma_1(\sigma_{ij}(\boldsymbol{\psi}(\boldsymbol{x}))n_j(\boldsymbol{x}))v_i^{(n)}(\boldsymbol{x})\,d\Gamma(\boldsymbol{x}) + \int_{\Gamma_2} p_i(\boldsymbol{x})\gamma_2 u_i^{(n)}(\boldsymbol{x})\,d\Gamma(\boldsymbol{x}) = \int_{\Gamma_2}\widetilde{t}_i(\boldsymbol{x})\gamma_2\psi_i(\boldsymbol{x})\,d\Gamma(\boldsymbol{x}). \quad (16)$$

Letting $n \to \infty$ in (16) we establish (11) and hence Lemma 1 is proved.

Now we are in a position to consider the variational problem. The first result concerning the approximate controllability is as follows.

THEOREM 1. *Let $\widetilde{\boldsymbol{t}} \in \mathbb{L}^2(\Gamma_2)$. If $\boldsymbol{v}$ varies in $\mathbb{L}^2(\Gamma_1)$, then $\gamma_2\boldsymbol{u}(\boldsymbol{v},\widetilde{\boldsymbol{t}})$ forms a dense set in $\mathbb{L}^2(\Gamma_2)$.*

Proof. Let $\boldsymbol{\eta} \in \mathbb{L}^2(\Gamma_2)$ be such that

$$\int_{\Gamma_2}\gamma_2 u_i(\boldsymbol{v},\widetilde{\boldsymbol{t}})\eta_i\,d\Gamma(\boldsymbol{x}) = 0 \qquad \forall\,\boldsymbol{v} \in \mathbb{L}^2(\Gamma_1). \quad (17)$$

Let $\boldsymbol{\psi}(\boldsymbol{0},\boldsymbol{\eta})$ be the solution of problem (10) with $\boldsymbol{p} = \boldsymbol{\eta}$. Then we have $\gamma_2\boldsymbol{\psi} \in \mathbb{L}^2(\Gamma_2)$. From Green's formula (11) and expression (17) we obtain

$$\int_{\Gamma_1}\gamma_1(\sigma_{ij}(\boldsymbol{\psi}(\boldsymbol{x}))n_j(\boldsymbol{x}))v_i(\boldsymbol{x})\,d\Gamma(\boldsymbol{x}) = \int_{\Gamma_2}\widetilde{t}_i(\boldsymbol{x})\gamma_2\psi_i(\boldsymbol{x})\,d\Gamma(\boldsymbol{x}) \qquad \forall\boldsymbol{v} \in \mathbb{L}^2(\Gamma_1). \quad (18)$$

Replacing $\boldsymbol{v}$ with $-\boldsymbol{v}$ in (18), we obtain

$$-\int_{\Gamma_1}\gamma_1(\sigma_{ij}(\boldsymbol{\psi}(\boldsymbol{x}))n_j(\boldsymbol{x}))v_i(\boldsymbol{x})\,d\Gamma(\boldsymbol{x}) = \int_{\Gamma_2}\widetilde{t}_i(\boldsymbol{x})\gamma_2\psi_i(\boldsymbol{x})\,d\Gamma(\boldsymbol{x}) \qquad \forall\boldsymbol{v} \in \mathbb{L}^2(\Gamma_1). \quad (19)$$

Equations (18) and (19) imply that

$$\int_{\Gamma_1}\gamma_1(\sigma_{ij}(\boldsymbol{\psi}(\boldsymbol{x}))n_j(\boldsymbol{x}))v_i(\boldsymbol{x})\,d\Gamma(\boldsymbol{x}) = 0 \qquad \forall\boldsymbol{v} \in \mathbb{L}^2(\Gamma_1)$$

and hence we have $\gamma_1(\sigma_{ij}(\boldsymbol{\psi}(\boldsymbol{x}))n_j(\boldsymbol{x})) = 0$ for $\boldsymbol{x} \in \Gamma_1$. Thus, $\boldsymbol{\psi} \in \mathbb{H}^{3/2}(\Omega)$ satisfies the problem given by (1) and the boundary conditions $\gamma_1\psi_i(\boldsymbol{x}) = \gamma_1(\sigma_{ij}(\boldsymbol{\psi}(\boldsymbol{x}))n_j(\boldsymbol{x})) = 0$, $\boldsymbol{x} \in \Gamma_1$. From a uniqueness theorem for the Cauchy problem in linear elasticity (**18**, Chapter 7, section 7.2; **19**), it follows that $\boldsymbol{\psi} \equiv \boldsymbol{0}$. Thus $\varepsilon(\boldsymbol{\psi}) \equiv \boldsymbol{0}$ and $\sigma(\boldsymbol{\psi}) \equiv \boldsymbol{0}$ in $\overline{\Omega}$ and therefore $\gamma_2(\sigma_{ij}(\boldsymbol{\psi}(\boldsymbol{x}))n_j(\boldsymbol{x})) = \eta_i(\boldsymbol{x}) = 0, \boldsymbol{x} \in \Gamma_2$. The theorem is proved.

This theorem has important consequences; for example, we can say that the Cauchy problem defined by (1) and (6) is solvable for almost all $\widetilde{\boldsymbol{u}}, \widetilde{\boldsymbol{t}} \in \mathbb{L}^2(\Gamma_2)$. Furthermore, we have the following result.

COROLLARY 1.

$$\inf_{\boldsymbol{v} \in \mathbb{L}^2(\Gamma_1)} J(\boldsymbol{v}) = 0.$$

THEOREM 2. *The functional $J(\boldsymbol{v})$ is twice Fréchet differentiable and is strictly convex. Moreover, its first gradient has the form*

$$J'(\boldsymbol{v}) = -\gamma_1(\sigma_{ij}(\boldsymbol{\psi}(\boldsymbol{x}))n_j(\boldsymbol{x})). \tag{20}$$

Proof. Let $\boldsymbol{h}$ be a vector-valued function in $\mathbb{L}^2(\Gamma_1)$ and denote by $\langle \cdot, \cdot \rangle_{\mathbb{L}^2(\Gamma_2)}$ the scalar product in the space $\mathbb{L}^2(\Gamma_2)$. Then using (8) and (9) we have

$$J(\boldsymbol{v}+\boldsymbol{h}) - J(\boldsymbol{v}) = \tfrac{1}{2}\|\gamma_2\boldsymbol{u}(\boldsymbol{v}+\boldsymbol{h}, \widetilde{\boldsymbol{t}}) - \widetilde{\boldsymbol{u}}\|^2_{\mathbb{L}^2(\Gamma_2)} - \tfrac{1}{2}\|\gamma_2\boldsymbol{u}(\boldsymbol{v}, \widetilde{\boldsymbol{t}}) - \widetilde{\boldsymbol{u}}\|^2_{\mathbb{L}^2(\Gamma_2)}. \tag{21}$$

The linearity of the boundary-value problems in elasticity implies the validity of the superposition principle, so that we have $\boldsymbol{u}(\boldsymbol{v}+\boldsymbol{h}, \widetilde{\boldsymbol{t}}) = \boldsymbol{u}(\boldsymbol{v}, \widetilde{\boldsymbol{t}}) + \boldsymbol{u}(\boldsymbol{h}, \boldsymbol{0})$, where $\boldsymbol{u}(\boldsymbol{h}, \boldsymbol{0})$ denotes the solution to the following direct problem:

$$\left.\begin{aligned} &\partial_j \sigma_{ij}(\boldsymbol{u}(\boldsymbol{x})) = 0, && \boldsymbol{x} \in \Omega, \\ &\gamma_1 u_i(\boldsymbol{x}) = h_i(\boldsymbol{x}), && \boldsymbol{x} \in \Gamma_1, \\ &\gamma_2(\sigma_{ij}(\boldsymbol{u}(\boldsymbol{x}))n_j(\boldsymbol{x})) = 0, && \boldsymbol{x} \in \Gamma_2. \end{aligned}\right\} \tag{22}$$

Thus (21) can be written in the following form:

$$\begin{aligned} J(\boldsymbol{v}+\boldsymbol{h}) - J(\boldsymbol{v}) &= \tfrac{1}{2}\|\gamma_2\boldsymbol{u}(\boldsymbol{v}, \widetilde{\boldsymbol{t}}) + \gamma_2\boldsymbol{u}(\boldsymbol{h}, \boldsymbol{0}) - \widetilde{\boldsymbol{u}}\|^2_{\mathbb{L}^2(\Gamma_2)} - \tfrac{1}{2}\|\gamma_2\boldsymbol{u}(\boldsymbol{v}, \widetilde{\boldsymbol{t}}) - \widetilde{\boldsymbol{u}}\|^2_{\mathbb{L}^2(\Gamma_2)} \\ &= \langle \gamma_2\boldsymbol{u}(\boldsymbol{v}, \widetilde{\boldsymbol{t}}) - \widetilde{\boldsymbol{u}}, \gamma_2\boldsymbol{u}(\boldsymbol{h}, \boldsymbol{0}) \rangle_{\mathbb{L}^2(\Gamma_2)} + \tfrac{1}{2}\|\gamma_2\boldsymbol{u}(\boldsymbol{h}, \boldsymbol{0})\|^2_{\mathbb{L}^2(\Gamma_2)}. \end{aligned} \tag{23}$$

Let us consider now the adjoint problem, namely

$$\left.\begin{aligned} &\partial_j \sigma_{ij}(\boldsymbol{\psi}(\boldsymbol{x})) = 0, && \boldsymbol{x} \in \Omega, \\ &\gamma_1 \psi_i(\boldsymbol{x}) = 0, && \boldsymbol{x} \in \Gamma_1, \\ &\gamma_2(\sigma_{ij}(\boldsymbol{\psi}(\boldsymbol{x}))n_j(\boldsymbol{x})) = \gamma_2(u_i(\boldsymbol{v}, \widetilde{\boldsymbol{t}})(\boldsymbol{x})) - \widetilde{u}_i(\boldsymbol{x}), && \boldsymbol{x} \in \Gamma_2. \end{aligned}\right\} \tag{24}$$

Applying Green's formula (11) to problems (22) and (24), we obtain

$$-\int_{\Gamma_1} \gamma_1(\sigma_{ij}(\boldsymbol{\psi}(\boldsymbol{x}))n_j(\boldsymbol{x}))h_i(\boldsymbol{x})\, d\Gamma(\boldsymbol{x}) = \int_{\Gamma_2} (\gamma_2(u_i(\boldsymbol{v}, \widetilde{\boldsymbol{t}})(\boldsymbol{x})) - \widetilde{u}_i(\boldsymbol{x}))\gamma_2 u_i(\boldsymbol{x})\, d\Gamma(\boldsymbol{x})$$

and, consequently, from (23) we have

$$J(\boldsymbol{v}+\boldsymbol{h}) - J(\boldsymbol{v}) = -\int_{\Gamma_1} \gamma_1(\sigma_{ij}(\boldsymbol{\psi}(\boldsymbol{x}))n_j(\boldsymbol{x}))h_i(\boldsymbol{x})\, d\Gamma(\boldsymbol{x}) + \tfrac{1}{2}\|\gamma_2\boldsymbol{u}(\boldsymbol{h}, \boldsymbol{0})\|^2_{\mathbb{L}^2(\Gamma_2)}. \tag{25}$$

Since $\boldsymbol{u}(\boldsymbol{h}, \boldsymbol{0})$ is the solution in $\mathbb{H}^{1/2}(\Omega)$ to problem (22), there exists a constant $c > 0$ such

that $\|\boldsymbol{u}(\boldsymbol{h},\boldsymbol{0})\|_{\mathbb{H}^{1/2}(\Omega)} \leqslant c\|\boldsymbol{h}\|_{\mathbb{L}^2(\Gamma_1)}$. It follows immediately that $\|\gamma_2\boldsymbol{u}(\boldsymbol{h},\boldsymbol{0})\|^2_{\mathbb{L}^2(\Gamma_2)} \to 0$ as $\|\boldsymbol{h}\|_{\mathbb{L}^2(\Gamma_1)} \to 0$ which means that the functional $J(\boldsymbol{v})$ is Fréchet differentiable and its first gradient is given by (20).

Consider now the problem

$$\left.\begin{aligned} &\partial_j\sigma_{ij}(\boldsymbol{\varphi}(\boldsymbol{x})) = 0, && \boldsymbol{x}\in\Omega,\\ &\gamma_1\varphi_i(\boldsymbol{x}) = 0, && \boldsymbol{x}\in\Gamma_1,\\ &\gamma_2(\sigma_{ij}(\boldsymbol{\varphi}(\boldsymbol{x}))n_j(\boldsymbol{x})) = \gamma_2(u_i(\boldsymbol{h},\boldsymbol{0})(\boldsymbol{x})), && \boldsymbol{x}\in\Gamma_2, \end{aligned}\right\} \tag{26}$$

which has a unique solution in $\mathbb{H}^{3/2}(\Omega)$ since $\gamma_2\boldsymbol{u}(\boldsymbol{h},\boldsymbol{0}) \in \mathbb{L}^2(\Gamma_2)$. If we apply Green's formula (11) to problems (22) and (26), we obtain

$$\int_{\Gamma_2} \gamma_2(u_i(\boldsymbol{h},\boldsymbol{0})(\boldsymbol{x}))\gamma_2(u_i(\boldsymbol{h},\boldsymbol{0})(\boldsymbol{x}))\,d\Gamma(\boldsymbol{x}) = -\int_{\Gamma_1} \gamma_1(\sigma_{ij}(\boldsymbol{\varphi}(\boldsymbol{x}))n_j(\boldsymbol{x}))h_i(\boldsymbol{x})\,d\Gamma(\boldsymbol{x}) \tag{27}$$

and it follows that the functional $J(\boldsymbol{v})$ is twice Fréchet differentiable and its second gradient is given by the formula

$$J''(\boldsymbol{v})\cdot\boldsymbol{h} = -\gamma_1(\sigma_{ij}(\boldsymbol{\varphi}(\boldsymbol{x}))n_j(\boldsymbol{x})).$$

In order to prove that the functional $J(\boldsymbol{v})$ is strictly convex, we first observe that $J(\boldsymbol{v})$ is convex since

$$\langle J''(\boldsymbol{v})\cdot\boldsymbol{h},\boldsymbol{h}\rangle_{\mathbb{L}^2(\Gamma_2)} = -\int_{\Gamma_1} \gamma_1(\sigma_{ij}(\boldsymbol{\varphi}(\boldsymbol{x}))n_j(\boldsymbol{x}))h_i(\boldsymbol{x})\,d\Gamma(\boldsymbol{x})$$

and, according to (27), we have

$$\langle J''(\boldsymbol{v})\cdot\boldsymbol{h},\boldsymbol{h}\rangle_{\mathbb{L}^2(\Gamma_2)} = \int_{\Gamma_2} |\gamma_2(u_i(\boldsymbol{h},\boldsymbol{0})(\boldsymbol{x}))|^2\,d\Gamma(\boldsymbol{x}) = \|\gamma_2(u_i(\boldsymbol{h},\boldsymbol{0})(\boldsymbol{x}))\|^2_{\mathbb{L}^2(\Gamma_2)} \geqslant 0.$$

Further, if $\langle J''(\boldsymbol{v})\cdot\boldsymbol{h},\boldsymbol{h}\rangle_{\mathbb{L}^2(\Gamma_2)} = 0$, then $\gamma_2(u_i(\boldsymbol{h},\boldsymbol{0})(\boldsymbol{x})) = 0$ and it follows that $\boldsymbol{u}(\boldsymbol{h},\boldsymbol{0})$ satisfies the problem

$$\left.\begin{aligned} &\partial_j\sigma_{ij}(\boldsymbol{u}(\boldsymbol{h},\boldsymbol{0})(\boldsymbol{x})) = 0, && \boldsymbol{x}\in\Omega,\\ &\gamma_2(u_i(\boldsymbol{h},\boldsymbol{0})(\boldsymbol{x})) = 0, && \boldsymbol{x}\in\Gamma_2,\\ &\gamma_2(\sigma_{ij}(\boldsymbol{u}(\boldsymbol{h},\boldsymbol{0})(\boldsymbol{x}))n_j(\boldsymbol{x})) = 0, && \boldsymbol{x}\in\Gamma_2. \end{aligned}\right\}$$

From a theorem on the uniqueness of the Cauchy problem in linear elasticity, we have that $\boldsymbol{u}(\boldsymbol{h},\boldsymbol{0}) \equiv \boldsymbol{0}$ in Ω. Hence $\boldsymbol{h} \equiv \boldsymbol{0}$ and the functional $J(\boldsymbol{v})$ is strictly convex.

4. Conjugate gradient method

As we can calculate the gradient of the functional $J(\boldsymbol{v})$ via the adjoint problem (24), we can now apply the CGM with a stopping rule, as proposed by Nemirovskii (**13**). First, we note that, by the superposition principle, $\boldsymbol{u}(\boldsymbol{v},\widetilde{\boldsymbol{t}}) = \boldsymbol{u}(\boldsymbol{v},\boldsymbol{0}) + \boldsymbol{u}(\boldsymbol{0},\widetilde{\boldsymbol{t}})$.

We define the linear operator

$$A_0\boldsymbol{v} := \gamma_2\boldsymbol{u}(\boldsymbol{v},\boldsymbol{0})$$

and thus we have the following linear equation, which is equivalent to (8):

$$A_0\boldsymbol{v} = \gamma_2(\boldsymbol{u}(\boldsymbol{v},\widetilde{\boldsymbol{t}}) - \boldsymbol{u}(\boldsymbol{0},\widetilde{\boldsymbol{t}})) = \gamma_2\boldsymbol{u}(\boldsymbol{v},\widetilde{\boldsymbol{t}}) - \gamma_2\boldsymbol{u}(\boldsymbol{0},\widetilde{\boldsymbol{t}}) = \widetilde{\boldsymbol{u}} - \gamma_2\boldsymbol{u}(\boldsymbol{0},\widetilde{\boldsymbol{t}}) =: \overline{\boldsymbol{u}}.$$

Suppose that instead of $\widetilde{\boldsymbol{u}}$ we have only an approximation, say $\widetilde{\boldsymbol{u}}_\varepsilon \in \mathbb{L}^2(\Gamma_2)$ such that

$$\|\widetilde{\boldsymbol{u}} - \widetilde{\boldsymbol{u}}_\varepsilon\|_{\mathbb{L}^2(\Gamma_2)} \leqslant \varepsilon. \tag{28}$$

In order to solve the Cauchy problem given by (1) and (6) with noisy data $\widetilde{\boldsymbol{u}}_\varepsilon$, we need to compute $A_0^*(A_0\boldsymbol{v} - \overline{\boldsymbol{u}}_\varepsilon)$, where A_0^* is the adjoint of the operator A_0 and $\overline{\boldsymbol{u}}_\varepsilon$ is given by

$$\overline{\boldsymbol{u}}_\varepsilon := \widetilde{\boldsymbol{u}}_\varepsilon - \gamma_2\boldsymbol{u}(\boldsymbol{v}, \boldsymbol{0}).$$

However, we observe that this is nothing else than the gradient (20) of the functional (9). Thus the CGM applied to our problem has the form of the following algorithm.

Step 1. Set $k = 0$. Choose $\boldsymbol{u}^{(0)} \in \mathbb{L}^2(\Gamma_2)$.

Step 2. Solve the direct problem

$$\left.\begin{aligned} &\partial_j\sigma_{ij}(\boldsymbol{u}(\boldsymbol{x})) = 0, && \boldsymbol{x} \in \Omega,\\ &\gamma_1 u_i(\boldsymbol{x}) = u_i^{(k)}(\boldsymbol{x}), && \boldsymbol{x} \in \Gamma_1,\\ &\gamma_2(\sigma_{ij}(\boldsymbol{u}(\boldsymbol{x}))n_j(\boldsymbol{x})) = \widetilde{t}_i(\boldsymbol{x}), && \boldsymbol{x} \in \Gamma_2, \end{aligned}\right\}$$

to determine the residual $\boldsymbol{r}^{(k)} = A\boldsymbol{u}^{(k)} - \widetilde{\boldsymbol{u}}_\varepsilon = \gamma_2\boldsymbol{u}(\boldsymbol{u}^{(k)}, \widetilde{\boldsymbol{t}}) - \widetilde{\boldsymbol{u}}_\varepsilon$.

Step 3. Solve the adjoint problem

$$\left.\begin{aligned} &\partial_j\sigma_{ij}(\psi(\boldsymbol{x})) = 0, && \boldsymbol{x} \in \Omega,\\ &\gamma_1\psi_i(\boldsymbol{x}) = 0, && \boldsymbol{x} \in \Gamma_1,\\ &\gamma_2(\sigma_{ij}(\psi(\boldsymbol{x}))n_j(\boldsymbol{x})) = r_i^{(k)}(\boldsymbol{x}), && \boldsymbol{x} \in \Gamma_2, \end{aligned}\right\}$$

to determine the gradient $\boldsymbol{g}^{(k)}$: $g_i^{(k)}(\boldsymbol{x}) = \gamma_1(\sigma_{ij}(\psi(\boldsymbol{0}, \boldsymbol{r}^{(k)})(\boldsymbol{x}))n_j(\boldsymbol{x}))$. Calculate β_k and $\boldsymbol{d}^{(k)}$ as follows:

$$k = 0 : \beta_k = 0, \qquad \boldsymbol{d}^{(k)} = -\boldsymbol{g}^{(k)},$$

$$k \geqslant 1 : \beta_k = \frac{\|\boldsymbol{g}^{(k)}\|^2_{\mathbb{L}^2(\Gamma_1)}}{\|\boldsymbol{g}^{(k-1)}\|^2_{\mathbb{L}^2(\Gamma_1)}}, \qquad \boldsymbol{d}^{(k)} = -\boldsymbol{g}^{(k)} + \beta_k\boldsymbol{d}^{(k-1)}.$$

Step 4. Solve the direct problem

$$\left.\begin{aligned} &\partial_j\sigma_{ij}(\boldsymbol{u}(\boldsymbol{x})) = 0, && \boldsymbol{x} \in \Omega,\\ &\gamma_1 u_i(\boldsymbol{x}) = d_i^{(k)}(\boldsymbol{x}), && \boldsymbol{x} \in \Gamma_1,\\ &\gamma_2(\sigma_{ij}(\boldsymbol{u}(\boldsymbol{x}))n_j(\boldsymbol{x})) = 0, && \boldsymbol{x} \in \Gamma_2, \end{aligned}\right\}$$

to determine $A_0\boldsymbol{d}^{(k)} = \gamma_2\boldsymbol{u}(\boldsymbol{d}^{(k)}, \boldsymbol{0})$. Compute α_k and $\boldsymbol{u}^{(k+1)}$ as follows:

$$\alpha_k = \frac{\|\boldsymbol{g}^{(k)}\|^2_{\mathbb{L}^2(\Gamma_1)}}{\|A_0\boldsymbol{d}^{(k)}\|^2_{\mathbb{L}^2(\Gamma_2)}}, \quad \boldsymbol{u}^{(k+1)} = \boldsymbol{r}^{(k)} + \alpha_k\boldsymbol{d}^{(k)}.$$

Step 5. Set $k = k + 1$. Repeat step 2 until a stopping criterion is achieved.

As a stopping criterion we choose the one suggested by Nemirovskii (**13**), namely choose the first $k \in \mathbb{N}$ such that

$$\|\boldsymbol{r}^{(k)}\|_{\mathbb{L}^2(\Gamma_2)} \leqslant \delta\varepsilon, \tag{29}$$

where $\delta > 1$ is a constant which can be taken heuristically to be 1·1, as suggested by Hanke and Hansen (**20**). It follows from Nemirovskii's result that the above iterative procedure converges with an optimal convergence rate to the exact solution of the problem as the noise level tends to zero.

We note that in step 2 we have the following relations:

$$\begin{aligned}\boldsymbol{r}^{(k+1)} &= A\boldsymbol{u}^{(k+1)} - \widetilde{\boldsymbol{u}}_\varepsilon = (A_0\boldsymbol{u}^{(k+1)} + \gamma_2\boldsymbol{u}(\boldsymbol{0}, \widetilde{\boldsymbol{t}})) - \widetilde{\boldsymbol{u}}_\varepsilon \\ &= A_0(\boldsymbol{u}^{(k)} + \alpha_k\boldsymbol{d}^{(k)}) + \gamma_2\boldsymbol{u}(\boldsymbol{0}, \widetilde{\boldsymbol{t}}) - \widetilde{\boldsymbol{u}}_\varepsilon = \alpha_k(A_0\boldsymbol{d}^{(k)}) + (A_0\boldsymbol{u}^{(k)} + \gamma_2\boldsymbol{u}(\boldsymbol{0}, \widetilde{\boldsymbol{t}})) - \widetilde{\boldsymbol{u}}_\varepsilon \\ &= \alpha_k(A_0\boldsymbol{d}^{(k)}) + A\boldsymbol{u}^{(k)} - \widetilde{\boldsymbol{u}}_\varepsilon = \alpha_k(A_0\boldsymbol{d}^{(k)}) + \boldsymbol{r}^{(k)}.\end{aligned}$$

Thus we obtain that $\boldsymbol{r}^{(k+1)} = \boldsymbol{r}^{(k)} + \alpha_k(A_0\boldsymbol{d}^{(k)})$ for $k \geqslant 0$ and we note that we have in fact to solve only the two direct problems in steps 3 and 4 at every iteration, except for that to determine $\boldsymbol{r}^{(0)}$.

5. Boundary element method

The Lamé system (5) in the two-dimensional case can be formulated in integral form with the aid of the Second Theorem of Betti (**21**), namely

$$C_{ij}(\boldsymbol{x})u_j(\boldsymbol{x}) + \int\!\!\!\!\!\!-_\Gamma T_{ij}(\boldsymbol{y}, \boldsymbol{x})u_j(\boldsymbol{y})\, d\Gamma(\boldsymbol{y}) = \int_\Gamma U_{ij}(\boldsymbol{y}, \boldsymbol{x})t_j(\boldsymbol{y})\, d\Gamma(\boldsymbol{y}) \tag{30}$$

for $i, j = 1, 2$, $\boldsymbol{x} \in \overline{\Omega} = \Omega \cup \Gamma$, and $\boldsymbol{y} \in \Gamma$, where the first integral is taken in the sense of the Cauchy principal value, $C_{ij}(\boldsymbol{x}) = 1$ for $\boldsymbol{x} \in \Omega$ and $C_{ij}(\boldsymbol{x}) = \frac{1}{2}$ for $\boldsymbol{x} \in \Gamma$ (smooth), and U_{ij} and T_{ij} are the fundamental displacements and tractions for the two-dimensional isotropic linear elasticity given by

$$\begin{aligned}U_{ij}(\boldsymbol{y}, \boldsymbol{x}) &= C_1\left(C_2\delta_{ij}\ln r(\boldsymbol{y}, \boldsymbol{x}) - \frac{\partial r(\boldsymbol{y}, \boldsymbol{x})}{\partial y_i}\frac{\partial r(\boldsymbol{y}, \boldsymbol{x})}{\partial y_j}\right), \\ T_{ij}(\boldsymbol{y}, \boldsymbol{x}) &= \frac{C_3}{r(\boldsymbol{y}, \boldsymbol{x})}\left[\left(C_4\delta_{ij} + 2\frac{\partial r(\boldsymbol{y}, \boldsymbol{x})}{\partial y_i}\frac{\partial r(\boldsymbol{y}, \boldsymbol{x})}{\partial y_j}\right)\frac{\partial r(\boldsymbol{y}, \boldsymbol{x})}{\partial n(\boldsymbol{y})}\right. \\ &\quad \left. - C_4\left(\frac{\partial r(\boldsymbol{y}, \boldsymbol{x})}{\partial y_i}n_j(\boldsymbol{y}) - \frac{\partial r(\boldsymbol{y}, \boldsymbol{x})}{\partial y_j}n_i(\boldsymbol{y})\right)\right].\end{aligned}$$

Here $r(\boldsymbol{y}, \boldsymbol{x})$ represents the distance between the collocation point $\boldsymbol{x}$ and the field point $\boldsymbol{y}$ and the constants C_1, C_2, C_3 and C_4 are given by $C_1 = -1/[8\pi G(1 - \overline{\nu})]$, $C_2 = 3 - 4\overline{\nu}$, $C_3 = -1/[4\pi(1 - \overline{\nu})]$ and $C_4 = 1 - 2\overline{\nu}$, where $\overline{\nu} = \nu$ for plane strain and $\overline{\nu} = \nu/(1 + \nu)$ for plane stress. It should be noted that in practice (30) can rarely be solved analytically and thus a numerical approximation is required. A BEM with constant boundary elements (**22**) is employed in order to solve the intermediate mixed well-posed boundary-value problems resulting from the iterative CGM adopted.

6. Numerical results and discussion

In this section we illustrate the numerical results obtained using the conjugate gradient and the BEMs according to the algorithm described in section 4. In addition we investigate the convergence of the algorithm with respect to the mesh size discretization and the number of iterations when the Cauchy data is exact and the stability of the algorithm when the Cauchy data is perturbed by noise.

6.1 *Example*

In order to present the performance of the numerical method proposed, we solve the Cauchy problem in a smooth geometry, namely the unit disc $\Omega = \{\boldsymbol{x} = (x_1, x_2) \,|\, x_1^2 + x_2^2 < 1\}$. We assume that the boundary $\Gamma = \{\boldsymbol{x} = (x_1, x_2) \,|\, x_1^2 + x_2^2 = 1\}$ of the solution domain Ω is divided into two disjoint parts, namely $\Gamma_1 = \{\boldsymbol{x} = (x_1, x_2) \,|\, \boldsymbol{x} \in \Gamma, \alpha_1 \leqslant \theta(\boldsymbol{x}) \leqslant \alpha_2\}$ and $\Gamma_2 = \{\boldsymbol{x} = (x_1, x_2) \,|\, \boldsymbol{x} \in \Gamma, 0 \leqslant \theta(\boldsymbol{x}) < \alpha_1\} \cup \{\boldsymbol{x} = (x_1, x_2) \,|\, \boldsymbol{x} \in \Gamma, \alpha_2 < \theta(\boldsymbol{x}) \leqslant 2\pi\}$, where $\theta(\boldsymbol{x})$ is the angular polar coordinate of $\boldsymbol{x}$ and α_i, $i = 1, 2$, are specified angles in the interval $(0, 2\pi)$. In order to illustrate typical numerical results we have taken $\alpha_1 = \pi/4$ and $\alpha_2 = 3\pi/4$ and we assume that Γ_2 is overspecified by the prescription of both the displacement and the traction vectors while Γ_1 is underspecified, with both the displacement and the traction vectors unknown.

We consider an isotropic linear elastic medium characterized by the material constants $G = 3{\cdot}35 \times 10^{10}$ N m^{-2} and $\nu = 0{\cdot}34$ corresponding to a copper alloy. The following analytical solution in displacements:

$$u_i^{(\mathrm{an})}(\boldsymbol{x}) = \frac{1 - \nu}{2G(1 + \nu)} \sigma_0 \, x_i, \qquad i = 1, 2, \tag{31}$$

in the domain Ω, corresponds to a uniform hydrostatic stress state given by

$$\sigma_{ij}^{(\mathrm{an})}(\boldsymbol{x}) = (\sigma_0/\overline{\sigma}) \, \delta_{ij}, \qquad i, j = 1, 2. \tag{32}$$

In (31) and (32), G and $\sigma_0 = 1{\cdot}5 \times 10^{10}$ N m^{-2} have been non-dimensionalized with $\overline{\sigma} = 10^{10}$ N m^{-2}. The Cauchy problem considered can be written as

$$\left.\begin{aligned} &\partial_j \sigma_{ij}(\boldsymbol{u}(\boldsymbol{x})) = 0, && \boldsymbol{x} \in \Omega, \\ &\sigma_{ij}(\boldsymbol{u}(\boldsymbol{x})) n_j(\boldsymbol{x}) = t_i^{(\mathrm{an})}(\boldsymbol{x}), && \boldsymbol{x} \in \Gamma_2, \\ &u_i(\boldsymbol{x}) = u_i^{(\mathrm{an})}(\boldsymbol{x}), && \boldsymbol{x} \in \Gamma_2, \end{aligned}\right\}$$

where $t_i^{(\mathrm{an})}(\boldsymbol{x}) = \sigma_{i1}^{(\mathrm{an})}(\boldsymbol{x}) n_1(\boldsymbol{x}) + \sigma_{i2}^{(\mathrm{an})}(\boldsymbol{x}) n_2(\boldsymbol{x})$ is the ith component of the traction vector $\boldsymbol{t}^{(\mathrm{an})} = (t_1^{(\mathrm{an})}, t_2^{(\mathrm{an})})$ corresponding to the uniform hydrostatic stress state (32).

6.2 *Initial guess*

An arbitrary vector-valued function $\boldsymbol{u}^{(0)} \in \mathbb{L}^2(\Gamma_1) \times \mathbb{L}^2(\Gamma_1)$ may be specified as an initial guess for the displacement vector on Γ_1, but in order to improve the rate of convergence of the iterative procedure we have chosen a vector-valued function which ensures the continuity of the displacement vector at the endpoints of Γ_1 and which is also linear with respect to the angular polar coordinate θ. For the test example considered, this initial guess is

$$u_i^{(0)}(\boldsymbol{x}) = \frac{\alpha_2 - \theta(\boldsymbol{x})}{\alpha_2 - \alpha_1} u_i^{(\mathrm{an})}(\boldsymbol{x_1}) + \frac{\theta(\boldsymbol{x}) - \alpha_1}{\alpha_2 - \alpha_1} u_i^{(\mathrm{an})}(\boldsymbol{x_2})$$

Table 1 Optimal iteration numbers and errors for $N \in \{40, 80, 160, 320\}$ boundary elements and input data $\boldsymbol{u}^{(\mathrm{an})}|_{\Gamma_2}$

N	40	80	160	320
ε	$3{\cdot}00 \times 10^{-3}$	$1{\cdot}28 \times 10^{-3}$	$5{\cdot}86 \times 10^{-4}$	$2{\cdot}78 \times 10^{-4}$
k_{opt}	5	5	15	41
$e_u(k_{\mathrm{opt}})$	$1{\cdot}00 \times 10^{-2}$	$8{\cdot}94 \times 10^{-3}$	$5{\cdot}04 \times 10^{-3}$	$4{\cdot}12 \times 10^{-3}$
$E_u(k_{\mathrm{opt}})$	$1{\cdot}43 \times 10^{-3}$	$4{\cdot}05 \times 10^{-4}$	$1{\cdot}75 \times 10^{-4}$	$5{\cdot}47 \times 10^{-5}$
k_N	2	2	5	5
$e_u(k_N)$	$1{\cdot}35 \times 10^{-2}$	$9{\cdot}19 \times 10^{-3}$	$5{\cdot}86 \times 10^{-3}$	$5{\cdot}14 \times 10^{-3}$
$E_u(k_N)$	$2{\cdot}60 \times 10^{-3}$	$1{\cdot}33 \times 10^{-3}$	$3{\cdot}34 \times 10^{-4}$	$2{\cdot}35 \times 10^{-4}$

for $i = 1, 2$, where $\alpha_i = \theta(\boldsymbol{x_i})$, $\boldsymbol{x_i}$ are the endpoints of Γ_1, and the choice of $\alpha_1 = \pi/4$ and $\alpha_2 = 3\pi/4$ also ensures that the initial guess is not too close to the exact values $u_i^{(\mathrm{an})}(\boldsymbol{x})$.

6.3 *Accuracy*

In order to investigate the convergence of the algorithm, at every iteration we evaluate the errors

$$e_u(k) = \|\boldsymbol{u}^{(k)} - \boldsymbol{u}^{(\mathrm{an})}\|_{\mathbb{L}^2(\Gamma_1)} \quad \text{and} \quad E_u(k) = \|A\boldsymbol{u}^{(k)} - \boldsymbol{u}^{(\mathrm{an})}\|_{\mathbb{L}^2(\Gamma_2)},$$

where $\boldsymbol{u}^{(k)}$ is the displacement vector on Γ_1 retrieved after k iterations, the operator A is given by (8) and each iteration consists of solving three direct mixed well-posed problems as described in section 4. These errors are plotted in Fig. 1 for various numbers of boundary elements $N \in \{40, 80, 160, 320\}$. From Fig. 1a it can be seen that the error e_u decreases up to a specific iteration after which it starts increasing. It should be noted that the pattern of the convergence process, with sharp decreases followed by flat portions, is common to conjugate gradient-type methods. The error E_u keeps decreasing as the number of iterations k increases, as can be seen in Fig. 1b, but there is a threshold of optimality at which the iterative process should be stopped according to Nemirovskii's rule.

In all the tables presented in this paper, ε represents the total amount of noise included in the input data, k_{opt} represents the optimal iteration number for which the accuracy norm e_u becomes a minimum, and k_N represents the optimal iteration number given by Nemirovskii's rule (29). Table 1 shows the optimal iteration numbers k_{opt} and k_N and the accuracy norms e_u and E_u for $N \in \{40, 80, 160, 320\}$ boundary elements when the analytical solution $\boldsymbol{u}^{(\mathrm{an})}|_{\Gamma_2}$ is used as additional data. In this case $\widetilde{\boldsymbol{u}} = \boldsymbol{u}^{(\mathrm{an})}|_{\Gamma_2}$, and $\widetilde{\boldsymbol{u}}_\varepsilon = \boldsymbol{u}_N^{(\mathrm{num})}|_{\Gamma_2}$ is the BEM numerical solution of the problem (33) with N boundary elements. Thus, in Table 1, $\varepsilon = \varepsilon(N) = \|\boldsymbol{u}^{(\mathrm{an})} - \boldsymbol{u}_N^{(\mathrm{num})}\|_{\mathbb{L}^2(\Gamma_2)}$. It can be observed that although the differences between k_{opt} and k_N increase as the number of boundary elements increases, the difference between the corresponding errors is small.

We note that the CGM algorithm described in section 4 is convergent as we increase the number of boundary elements, as can be seen in Fig. 2 which presents the evolution of the numerical solution

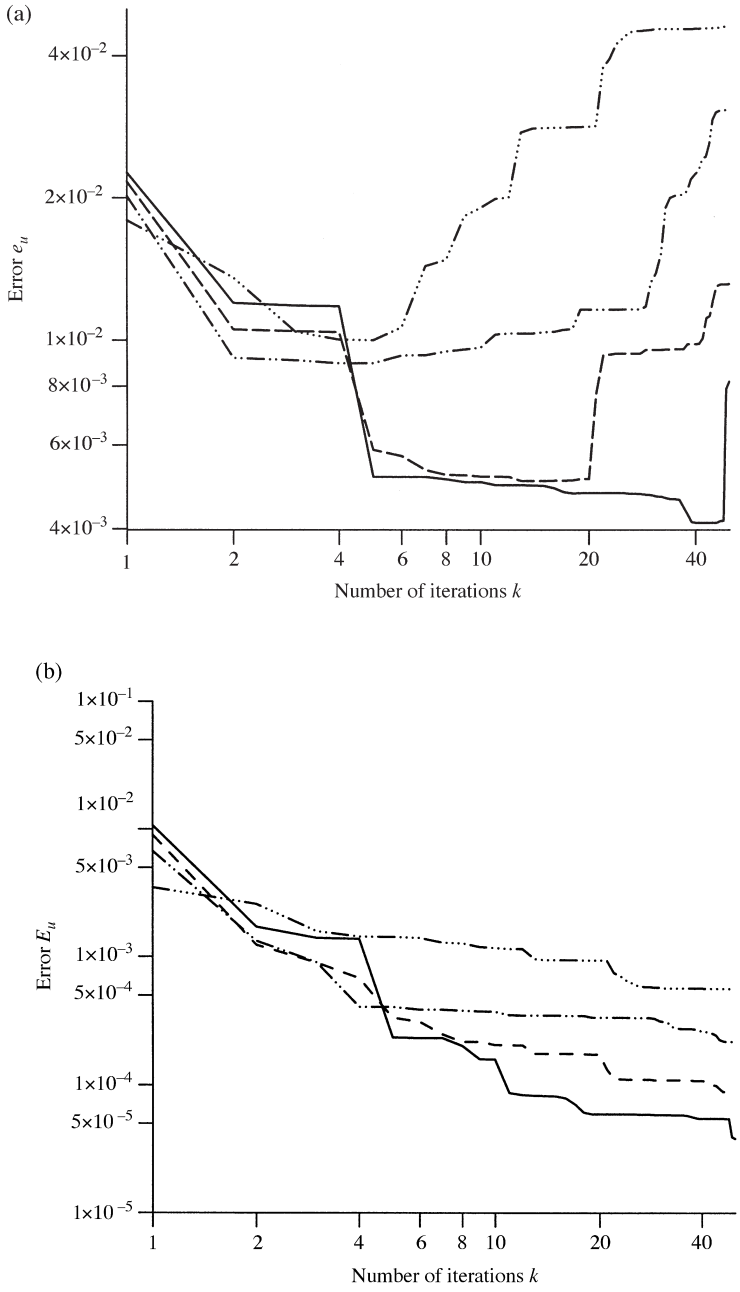

Fig. 1 (a) The error e_u obtained for $N = 40$ ($- \cdots - \cdots -$), $N = 80$ ($- \cdots -$), $N = 160$ ($- -$) and $N = 320$ (—) boundary elements and input data $\boldsymbol{u}^{(\mathrm{an})}|_{\Gamma_2}$. (b) The error E_u retrieved for $N = 40$ ($- \cdots - \cdots -$), $N = 80$ ($- \cdots -$), $N = 160$ ($- -$) and $N = 320$ (—) boundary elements and input data $\boldsymbol{u}^{(\mathrm{an})}|_{\Gamma_2}$

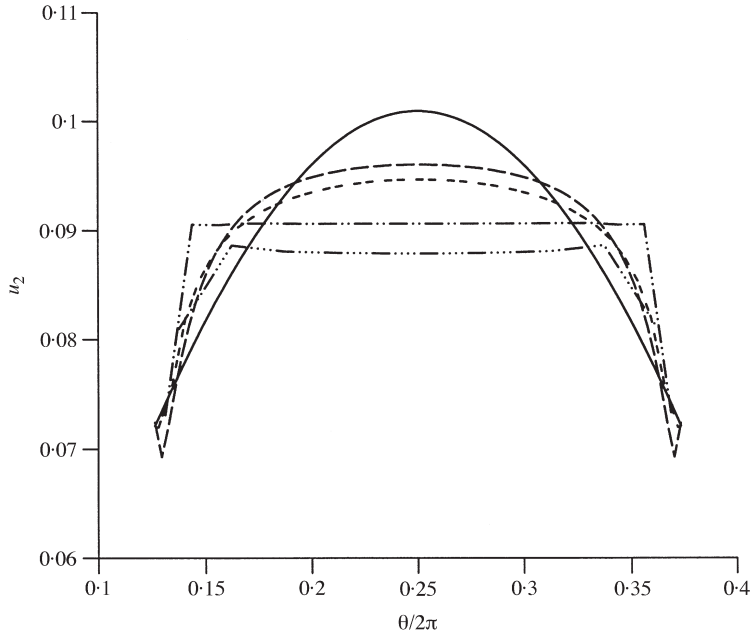

Fig. 2 The analytical solution $u_2^{(\mathrm{an})}|_{\Gamma_1}$ (—) and the numerical solution $u_2^{(\mathrm{num})}|_{\Gamma_1}$ obtained for $N = 40$ (– · · · · –), $N = 80$ (– · · –), $N = 160$ (– – ––) and $N = 320$ (— —) boundary elements and input data $\boldsymbol{u}^{(\mathrm{an})}|_{\Gamma_2}$

for the x_2 component of the displacement on Γ_1 for various numbers of boundary elements $N \in \{40, 80, 160, 320\}$. The behaviour of the x_1 component of the displacement vector is similar to that of the x_2 component and therefore it has not been presented here. It should be noted that as N increases, ε decreases and the numerical solution approximates better the exact solution, and hence the errors decrease as expected. However, the errors in predicting $\boldsymbol{t}$ on the underspecified boundary Γ_1 are still large since we are using as input data the analytical $\boldsymbol{u}^{(\mathrm{an})}|_{\Gamma_2}$ which is contaminated by numerical noise.

An alternative way to generate the Cauchy data on Γ_2 is to use the numerical solution $\boldsymbol{u}^{(\mathrm{num})}|_{\Gamma_2}$ of the direct problem

$$\left.\begin{aligned} &\partial_j \sigma_{ij}(\boldsymbol{u}\boldsymbol{x})) = 0, && \boldsymbol{x} \in \Omega, \\ &\gamma_1 u_i(\boldsymbol{x}) = u_i^{(\mathrm{an})}(\boldsymbol{x}), && \boldsymbol{x} \in \Gamma_1, \\ &\gamma_2(\sigma_{ij}(\boldsymbol{u}(\boldsymbol{x}))n_j(\boldsymbol{x})) = t_i^{(\mathrm{an})}(\boldsymbol{x}), && \boldsymbol{x} \in \Gamma_2, \end{aligned}\right\} \tag{33}$$

and this procedure can also be used to fabricate the input data when no exact solution to the Cauchy problem is available. In this case both e_u and E_u decrease as the number of iterations k increases

(Fig. 3), and the sequence $\{\boldsymbol{u}^{(k)}\}_{k\geqslant 0}$ of approximation functions for $\boldsymbol{u}|_{\Gamma_1}$ converges exactly to the analytical solution $\boldsymbol{u}^{(\mathrm{an})}|_{\Gamma_1}$, as can be seen in Fig. 4. However, the numerical solution for the traction vector deviates from the exact solution, especially near the ends of the underspecified boundary Γ_1, where the constant BEM changes to mixed boundary conditions and, therefore, it has not been presented here. Similar results have been reported in (**12**) for the heat flux in the case of the conjugate gradient–boundary element solution to the Cauchy problem for Laplace's equation. It is well known (**23**, **24**) that the gradient of the displacement vector $\boldsymbol{u}$ possesses singularities at the boundary points, where the data changes from displacement boundary conditions to traction boundary conditions, even if the displacement and the traction data are of class C^{∞}. Consequently, the classical solution for the displacement vector $\boldsymbol{u}$ cannot be smooth, although its smoothness can be improved if the displacement and the traction data are required to satisfy an increasing number (increasing with smoothness) of additional conditions; see also (**25**). Nevertheless, in the numerical implementation one may use linear boundary elements to enforce a smooth displacement across the junctions $\overline{\Gamma}_1 \cap \overline{\Gamma}_2$ and this will be investigated in a future work. In any case, retrieving higher-order derivatives (tractions) from noisy lower-order derivatives (displacements) is in itself an unstable problem and regularization procedures, such as the truncated singular value decomposition (TSVD) (**26**), can be employed. Alternatively, the inclusion of a relaxation factor in the iterative CGM is investigated next.

6.4 *Variable relaxation factor*

Here we investigate the relaxation marching condition

$$\boldsymbol{u}^{(k+1)} = \rho(\boldsymbol{r}^{(k)} + \alpha_k \boldsymbol{d}^{(k)}) + (1-\rho)\boldsymbol{u}^{(k)} \tag{34}$$

when passing from step 4 to step 5 of the algorithm described in section 4, where ρ is a relaxation parameter to be prescribed.

By a thorough inspection of the numerical solution for the displacement vector on Γ_1, obtained after various numbers of iterations without relaxation, we noticed at the endpoints of the underspecified boundary that the rate of convergence is higher than elsewhere on Γ_1. The high rate of movement of the numerical displacement at the endpoints of Γ_1, in comparison with its rate of movement elsewhere on the underspecified boundary, suggests the introduction of a variable relaxation factor $\rho = \rho(\theta(\boldsymbol{x}))$ which is small at the endpoints of Γ_1 and has a maximum value, say A, in the middle of Γ_1, which is the region of the highest ill-posedness, that is, the farthest away from Γ_2 where the Cauchy data is prescribed. Based on this discussion, for the circular geometry considered in section 6.1, the variable relaxation factor was chosen as (**27**)

$$\rho(\theta(\boldsymbol{x})) = A \sin \pi \left(\frac{\theta(\boldsymbol{x}) - \alpha_1}{\alpha_2 - \alpha_1} \right), \tag{35}$$

where $A \in (0, 2]$. In all the following figures and tables, we present more accurate estimates of the solution obtained using the variable relaxation factor given by (35) with $A = 2{\cdot}0$, although similar results can be obtained with $A \in (0, 2]$.

It should be mentioned that unlike in Fig. 1, when using the variable relaxation factor given by (35), both e_u and E_u decrease smoothly as the number of iterations k increases; see Fig. 5. Although not illustrated, it is reported that when k is sufficiently large then the error e_u shown in Fig. 5a for $N = 160$ will become smaller than the error e_u for $N = 80$; similarly for the error E_u

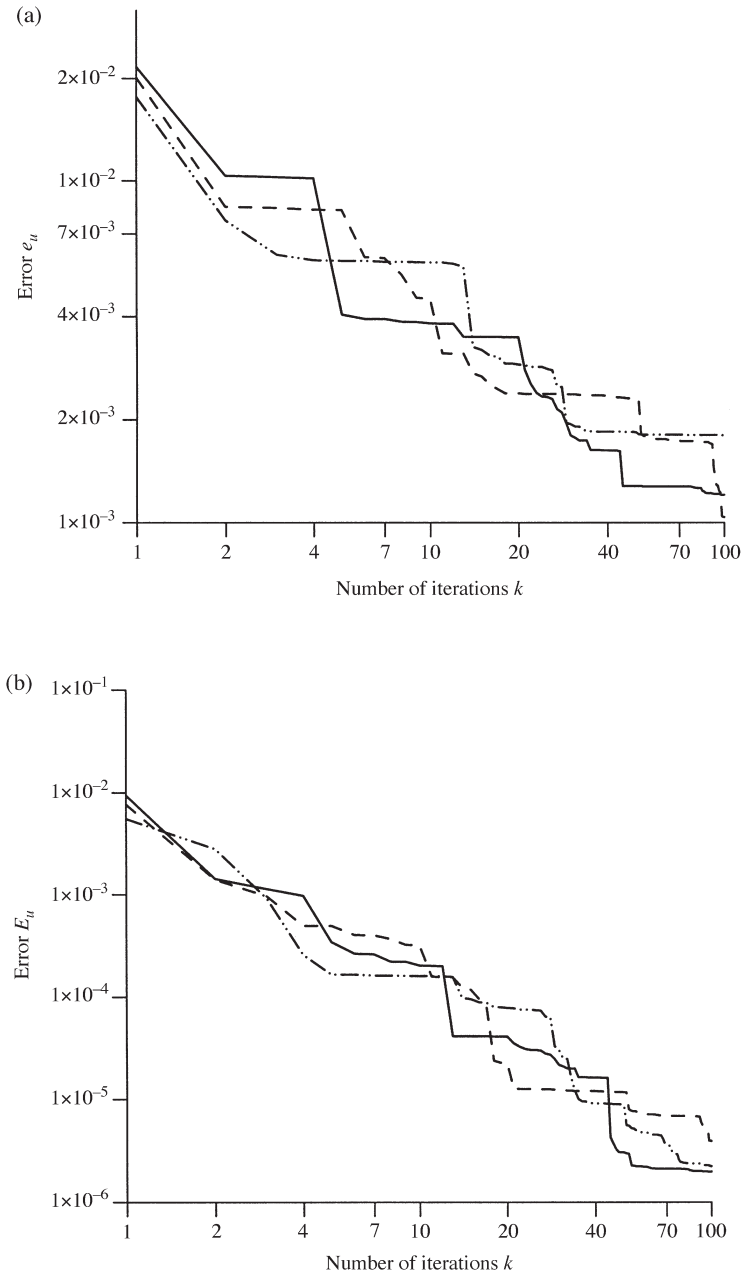

Fig. 3 (a) The error e_u obtained for $N = 40$ ($- \cdot \cdot -$), $N = 80$ ($--$) and $N = 160$ (—) boundary elements and input data $\boldsymbol{u}^{(\text{num})}|_{\Gamma_2}$. (b) The error E_u obtained for $N = 40$ ($- \cdot \cdot -$), $N = 80$ ($--$) and $N = 160$ (—) boundary elements and input data $\boldsymbol{u}^{(\text{num})}|_{\Gamma_2}$

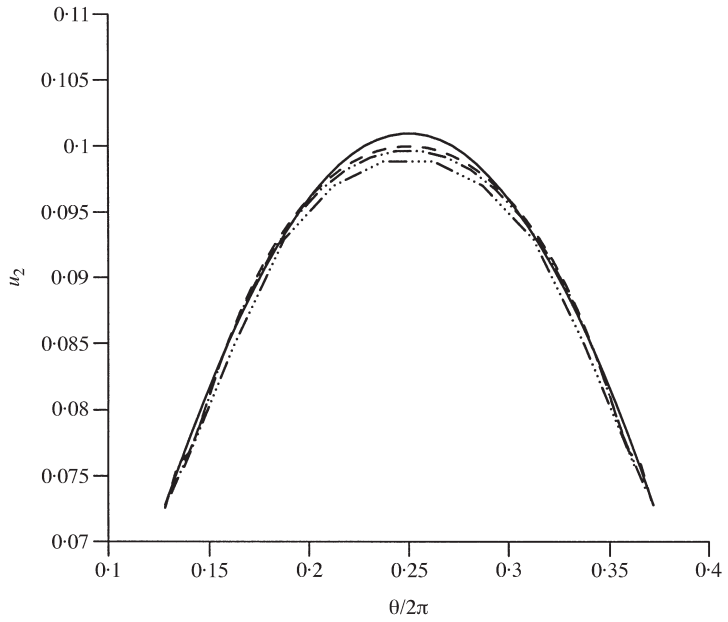

Fig. 4 The analytical solution $u_2^{(an)}|_{\Gamma_1}$ (—) and the numerical solution $u_2^{(num)}|_{\Gamma_1}$ obtained for $N = 40$ $(- \cdots -)$, $N = 80$ $(- \cdot -)$ and $N = 160$ $(--)$ boundary elements and input data $\boldsymbol{u}^{(num)}|_{\Gamma_2}$

(Fig. 5b). Table 2 shows the optimal iteration number k_N according to the stopping criterion (29) for $N \in \{40, 80, 160\}$ boundary elements and variable relaxation factor with amplitude $A = 2{\cdot}0$ when the analytical solution $\boldsymbol{u}^{(an)}|_{\Gamma_2}$ is used as additional data. From Tables 1 and 2 it can be seen that e_u is smaller and, consequently, the numerical solution $\boldsymbol{u}^{(num)}|_{\Gamma_1}$ approximates better the exact solution $\boldsymbol{u}^{(an)}|_{\Gamma_1}$ when using the variable relaxation factor (35). However, since E_u is larger it follows that more iterations are needed before the algorithm is stopped. This improvement in accuracy can be seen by comparing Figs 2 and 6. This comparison also shows that the numerical solution becomes smoother when relaxation is used. Finally, from both Figs 2 and 6 it can be seen that the numerical solution is convergent to the exact solution as N increases.

6.5 *Stability of the algorithm*

The stability of the numerical method proposed has been investigated by perturbing the initial data $\boldsymbol{u}|_{\Gamma_2}$ as $u_i = u_i + \delta u_i$, where δu_i is a Gaussian random variable with mean zero and standard deviation $\sigma = (p/100) \max_{\Gamma_2} |u_i|$, generated by the NAG subroutine G05DDF, and p is the percentage of additive noise included in the input data $\boldsymbol{u}|_{\Gamma_2}$ in order to simulate the inherent measurements errors.

Figure 7 shows the numerical displacement $u_2^{(num)}|_{\Gamma_1}$ obtained for $N = 80$ and variable relaxation

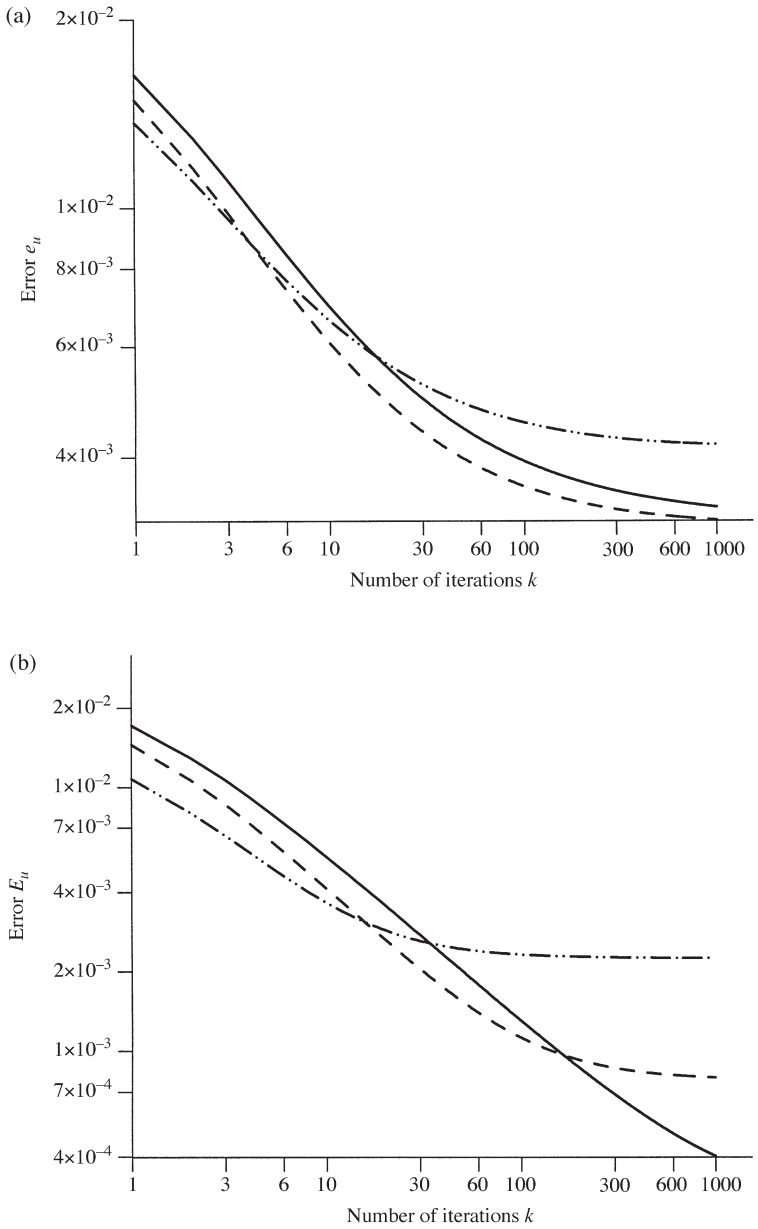

Fig. 5 (a) The error e_u obtained for $N = 40$ ($- \cdot \cdot -$), $N = 80$ ($--$) and $N = 160$ (—) boundary elements, variable relaxation factor with amplitude $A = 2{\cdot}0$ and input data $\boldsymbol{u}^{(\mathrm{an})}|_{\Gamma_2}$. (b) The error E_u obtained for $N = 40$ ($- \cdot \cdot -$), $N = 80$ ($--$) and $N = 160$ (—) boundary elements, variable relaxation factor with amplitude $A = 2{\cdot}0$ and input data $\boldsymbol{u}^{(\mathrm{an})}|_{\Gamma_2}$

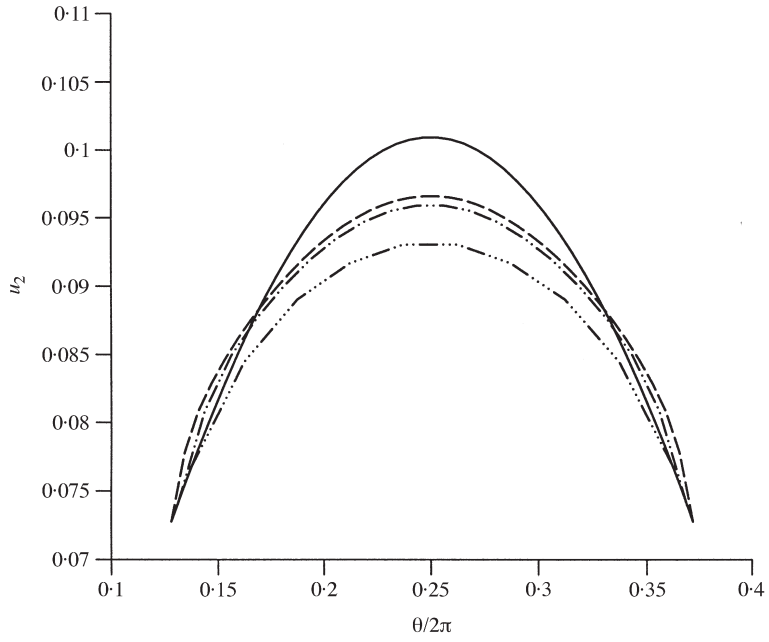

Fig. 6 The analytical solution $u_2^{(\mathrm{an})}|_{\Gamma_1}$ (—) and the numerical solution $u_2^{(\mathrm{num})}|_{\Gamma_1}$ obtained for $N = 40$ ($- \cdots - \cdots -$), $N = 80$ ($- \cdots -$) and $N = 160$ ($--$) boundary elements, variable relaxation factor with amplitude $A = 2{\cdot}0$ and input data $\boldsymbol{u}^{(\mathrm{an})}|_{\Gamma_2}$

factor (35) with $A = 2{\cdot}0$, when the Cauchy data on Γ_2 is taken to be the numerical solution $\boldsymbol{u}^{(\mathrm{num})}|_{\Gamma_2}$ of the direct problem (33) to which various amounts of noise $p \in \{0, 1, 2\}$ have been added. From this figure and from the optimal iteration numbers and the errors presented in Table 3, it can be seen that as p decreases the numerical solution approximates better the exact solution, whilst at the same time remaining stable.

7. Conclusions

In this paper we have formulated the Cauchy problem for the Lamé system in a variational form where only weak requirements for the Cauchy data are required. Consequently, the solution of the direct problems, as well as the associated adjoint problems, are defined in a weak sense and a mathematical analysis has been undertaken. The variational approach for solving the Cauchy problem in elasticity needs the gradient of the minimization functional, which is provided by the solution of the adjoint problem.

Due to the explicit representation of the gradient, the CGM was employed to solve the Cauchy problem numerically. The algorithm proposed consists of solving three direct mixed well-posed problems for the Lamé system at every iteration but because of the linearity of the problem only

Table 2 Optimal iteration numbers and errors for $N \in \{40, 80, 160\}$ boundary elements, variable relaxation factor with amplitude $A = 2{\cdot}0$ and input data $\boldsymbol{u}^{(\mathrm{an})}|_{\Gamma_2}$

N	40	80	160
ε	$3{\cdot}00 \times 10^{-3}$	$1{\cdot}28 \times 10^{-3}$	$5{\cdot}86 \times 10^{-4}$
k_N	13	59	337
$e_u(k_N)$	$6{\cdot}17 \times 10^{-3}$	$3{\cdot}85 \times 10^{-3}$	$3{\cdot}50 \times 10^{-3}$
$E_u(k_N)$	$3{\cdot}29 \times 10^{-3}$	$1{\cdot}41 \times 10^{-3}$	$6{\cdot}44 \times 10^{-4}$

Table 3 Optimal iteration numbers and errors for $N = 80$ boundary elements, variable relaxation factor with amplitude $A = 2{\cdot}0$ and various amounts $p \in \{0, 1, 2\}$ of noise added into the input data $\boldsymbol{u}^{(\mathrm{num})}|_{\Gamma_2}$

p	0%	1%	2%
ε	0·00	$2{\cdot}73 \times 10^{-3}$	$5{\cdot}58 \times 10^{-3}$
k_N	∞	60	24
$e_u(k_N)$	$2{\cdot}42 \times 10^{-3}$	$3{\cdot}21 \times 10^{-3}$	$6{\cdot}11 \times 10^{-3}$
$E_u(k_N)$	$4{\cdot}13 \times 10^{-4}$	$3{\cdot}06 \times 10^{-3}$	$4{\cdot}09 \times 10^{-3}$

two direct solutions are required at every iteration. In combination with Nemirovskii's stopping criterion, the CGM is known to be of optimal order when the data is sufficiently smooth. The use of a variable relaxation factor increased the accuracy of the numerical solution. The numerical implementation of the CGM is accomplished by using the BEM, which requires the discretization of the boundary only. Cauchy problems are inverse boundary-value problems and thus the BEM is a very suitable method for solving such improperly posed problems.

From the discussion of the results obtained for a typical example, it can be concluded that the CGM with an appropriate stopping rule together with the BEM produce a convergent, stable and consistent numerical solution with respect to increasing the number of boundary elements and decreasing the amount of noise added into the input Cauchy data.

Acknowledgements

The first author would like to acknowledge financial support received from the ORS and the Department of Applied Mathematics at the University of Leeds. The second author would like to thank the Royal Society and the Alexander von Humboldt Foundation for supporting his visits to the University of Leeds and the Wolfgang Goethe University Frankfurt am Main, respectively. The authors would like to thank Dr L. Elliott and Professor D. B. Ingham from the Department

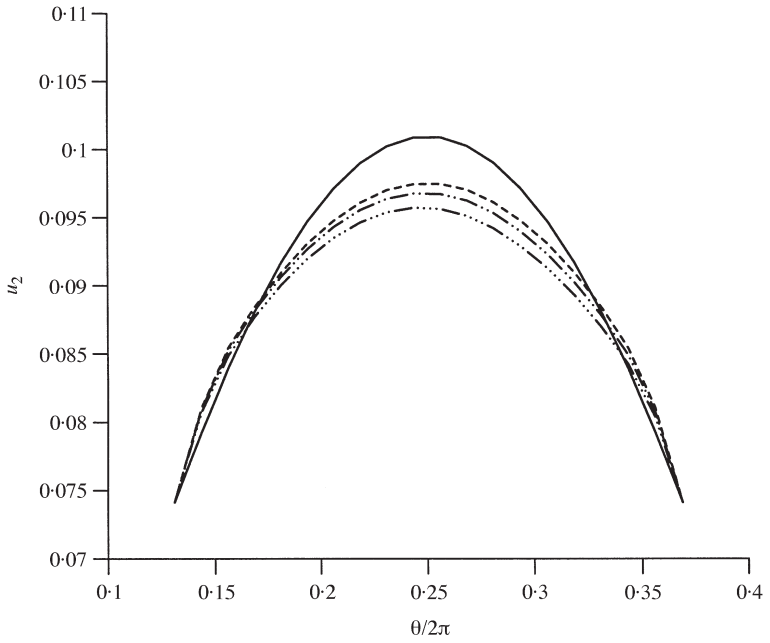

Fig. 7 The analytical solution $u_2^{(an)}|_{\Gamma_1}$ (—) and the numerical solution $u_2^{(num)}|_{\Gamma_1}$ obtained for $N = 80$ boundary elements, variable relaxation factor with the amplitude $A = 2{\cdot}0$ and various amounts of noise $p = 0\%$ (−−), $p = 1\%$ (− · · −) and $p = 2\%$ (− · · · · −) added into the input data $\boldsymbol{u}^{(num)}|_{\Gamma_2}$

of Applied Mathematics at the University of Leeds for all their encouragement in performing this research work.

References

1. J. V. Beck, B. Blackwell and C. R. St Clair, *Inverse Heat Conduction: Ill-posed Problems* (Wiley-Interscience, New York 1985).
2. K. Grysa, J. Cialkowski and H. Kaminski, An inverse temperature field problem of the theory of thermal stresses, *Nucl. Eng. Des.* **64** (1981) 169–184.
3. T. Mura, A new NDT: evaluation of plastic strain in bulk from displacements on surfaces, *Mech. Res. Commun.* **12** (1985) 243–248.
4. A. Maniatty, N. Zabaras and K. Stelson, Finite element analysis of some elasticity problems, *J. Eng. Mech.* **115** (1989) 1302–1316.
5. N. Zabaras, V. Morellas and D. Schnur, Spatially regularized solution of inverse elasticity problems using the BEM, *Commun. Appl. Numer. Meth.* **5** (1989) 547–553.
6. D. Schnur and N. Zabaras, Finite element solution of two-dimensional elastic problems using spatial smoothing, *Int. J. Numer. Meth. Eng.* **30** (1990) 57–75.

7. M. Ikehata, An inverse problem for the plate in the Love–Kirchhoff theory, *SIAM J. Appl. Math.* **53** (1993) 942–970.
8. F. Zhang, A. J. Kassab and D. W. Nicholson, A boundary element inverse approach for determining the residual stress and contact pressure, *Boundary Elements* XVII (ed. C. A. Brebbia *et al.*; WIT Press, Southampton, Boston 1995) 331–338.
9. X. Shi and S. Mukherjee, Shape optimization in three-dimensional linear elasticity by the boundary countour method, *Eng. Anal. Bound. Elem.* **23** (1999) 627–637.
10. S. Kubo, Inverse problems related to the mechanics and fracture of solids and structures, *JSME Int. J.* **31** (1988) 157–166.
11. V. G. Yakhno, *Inverse Problems for Differential Equations of Elasticity* (Novosibirsk, Nauka Sibirsk. Otdel 1990) (Russian).
12. Dinh Nho Hào and D. Lesnic, The Cauchy problem for Laplace's equation via the conjugate gradient method, *IMA J. Appl. Math.* **65** (2000) 199–217.
13. A. S. Nemirovskii, The regularizing properties of the adjoint gradient method in ill-posed problems, *USSR Comput. Maths Math. Phys.* **26**, 2 (1986) 7–16.
14. C. H. Huang and W. Y. Shih, A boundary element based solution of an inverse elasticity problem by conjugate gradient and regularization method, *Proc. 7th Int. Offshore Polar Eng. Conf.* (Honolulu, USA 1997) 388–395.
15. A. S. Saada, *Elasticity: Theory and Applications* (Pergamon Press, New York 1974).
16. J. Hadamard, *Lectures on Cauchy's Problem in Linear Partial Differential Equations* (Oxford University Press, London 1923).
17. J. L. Lions and E. Magenes, *Non-homogeneous Boundary Value Problems and their Applications*, Vol. 1 (Springer, Berlin 1972).
18. R. J. Knops and L. E. Payne, *Uniqueness Theorems in Linear Elasticity* (Springer, Berlin 1971).
19. G. Alessandrini and A. Morassi, Strong unique continuation for the Lamé system of elasticity, *Commun. Partial Diff. Equ.* to appear.
20. M. Hanke and P. C. Hansen, Regularization methods for large-scale problems, *Surv. Math. Ind.* **3** (1993) 253–315.
21. C. A. Brebbia, J. F. C. Telles and L. C. Wrobel, *Boundary Element Techniques: Theory and Application in Engineering* (Springer, Berlin 1984).
22. L. Marin, L. Elliott, D. B. Ingham and D. Lesnic, Boundary element solution for the Cauchy problem in linear elasticity, *Boundary Elements* XXII (ed. C. A. Brebbia and H. Power; WIT Press, Southampton, Boston 2000) 83–92.
23. G. Fichera, Sul problema della derivata obliqua e sul problema misto per l'equazione di Laplace, *Boll. Un. Mat. Ital.* **7** (1952) 367–377.
24. P. Schiavone, Mixed problems in the theory of elastic plates with transverse shear deformation, *Q. Jl Mech. Appl. Math.* **50** (1997) 239–249.
25. W. L. Wendland, E. Stephan and G. C. Hsiao, On the integral equation method for the plane mixed boundary value problem for the Laplacian, *Math. Meth. Appl. Sci.* **1** (1979) 265–321.
26. D. Lesnic, L. Elliott and D. B. Ingham, The boundary element solution of the Laplace and biharmonic equations subjected to noisy boundary data, *Int. J. Numer. Meth. Eng.* **42** (1998) 479–492.
27. N. S. Mera, L. Elliott, D. B. Ingham and D. Lesnic, The effect of a variable relaxation factor on the rate of convergence in the Cauchy problem, *Boundary Element Techniques* (ed. M. H Aliabadi; Queen Mary and Westfield College, University of London, London 1999) 357–366.